https://doi.org/10.48048/tis.2023.5284

THz Field Enhancement under the Influence of Cross-focused Laser Beams in the m-CNTs

Vishal Thakur, Niti Kant and Sandeep Kumar*

Department of Physics, Lovely Professional University, Phagwara 144411, Punjab, India

(*Corresponding author's e-mail: sanphymagic@gmail.com)

Received: 18 July 2022, Revised: 18 August 2022, Accepted: 25 August 2022, Published: 15 March 2023

Abstract

In the present analysis, we have studied the effect of cross-focused Gaussian laser beams propagating through the array of magnetized carbon nanotubes (m-CNTs) to enhance the terahertz (THz) field amplitude of emitted radiation. The plasma present in the form of CNTs rearranges itself due to the ponderomotive nonlinearity, which gives rise to the nonlinear optical phenomenon known as the cross-focusing of laser beams. The ponderomotive nonlinearity, cross-focusing of lasers, and anharmonic behavior of m-CNTs are responsible for the very strong nonlinear current density in the system. The cross-focusing effect of the propagating Gaussian laser beams increases with the increase in the externally applied static magnetic field, which is applied along the longitudinal axis of the CNTs. As a result, the normalized THz field amplitude shows a significant enhancement, and the THz radiations emitted in this way can be utilized in biological diagnosis (of the living beings) instead of X-rays. The internal and external diameters of the CNTs also make a notable impact on the THz field amplitude.

Keywords: THz field amplitude, Magnetized CNTs, Cross-focusing, Anharmonic behavior, Static magnetic field

List of abbreviations

THz: Terahertz
CNTs: Carbon Nanotubes
SWCNTs: Single-Walled Carbon Nanotubes
m-CNTs: Magnetized Carbon Nanotubes

Introduction

THz science and technology have been explored by many research workers to open up new doors for research opportunities in various promising domains like pharmaceutical and biological sciences [1-3], THz spectroscopy and imaging [4], and broadband communication and data transfer techniques [5]. For efficient THz generation, the research workers formulated various schemes. The researchers preferred the CNTs under the influence of an external magnetic field to generate efficient THz radiation [6-9]. This is because of some special features of CNTs like high thermal and electrical conductivity with nano dimensions. Thakur *et al.* and Kumar *et al.* [10,11] employed anharmonic CNTs to generate THz radiation. The SWCNTs are preferred by Titova *et al.* [12] for THz generation by using a filamented laser beam. The filamentation under the influence of various fields also provides efficient THz generation [13-16]. The cross-focusing of laser beams in collisional plasma under the influence of various fields made a deep impact on the THz radiation [17-21]. It was observed that in cross-focusing, one laser beam follows the other and vice versa such that focusing of one affects the other. In the present work, we are using the cross-focusing effect of laser beams in the array of m-CNTs to provide a novel scheme to generate compact, efficient, cost-effective, and energetic sources of THz radiation.

In this theoretical work of THz generation, we irradiate 2 cross-focused laser beams on the array of m-CNTs embedded in glass substrate (obtained by synthesizing with the plasma-enhanced chemical vapor deposition). The CNTs are known as magnetized CNTs under the effect of an external magnetic field (B). In the present case, the magnetic field is applied (y-direction) mutually perpendicular to the direction of co-propagation (z-direction) and polarization of laser beams (x-direction). In the array, each grown CNT has the following characteristics: Inner radius a_1, outer radius a_2 and length l_c. The plasma frequency associated with CNTs in terms of free electron density (n_0) can be expressed as $\omega_P = (n_0 e^2/m\varepsilon_0)^{1/2}$, where e and m represent the charge and mass of the electron. The number density of

CNTs in terms of the carbon nanotube separation (d) is given by the relation $N_c = 1/d^2$. In this scheme, we have used an array of CNTs in the form of plasma (preformed plasma). The ponderomotive force acts on the electrons of CNTs to produce nonlinearity and the plasma of CNTs gets rearranges itself along the direction of the external magnetic field. This ponderomotive nonlinearity is accountable for the cross-focusing of laser beams in the m-CNTs. The paper has been well arranged in 4 parts. In part-I, we have provided the introduction and significance of the research work. In part II of the paper, we explain the cross-focusing phenomenon of 2 Gaussian laser beams in the m-CNTs. In part III, we have provided the theoretical model for the generation of THz radiation. In part IV of the paper, the discussion is summarized with the conclusion.

Cross focusing of lasers beams in m-CNTs

In this novel scheme, consider 2 linearly polarized Gaussian laser beams co-propagating along z-direction in the plasma present in the form of m-CNTs with frequencies (ω_1, ω_2) and wavenumbers (k_1, k_2). The electric and magnetic field profiles associated with propagating laser beams can be expressed in terms of the amplitude of electric fields (E_{jx0}), wavenumber (k_j) and dielectric function of plasma (ϵ_j) written as:

$$\vec{E}_j = \hat{x}E_{jx0}\exp\{-i(k_j z - \omega_j t)\}; \; j=1, 2, \tag{1}$$

$$\vec{B}_j = ic(\vec{\nabla} \times \vec{E}_j)/\omega_j, \tag{2}$$

where, the dielectric function in terms of relative permittivity of the lattice is given by the relation $\epsilon_j = \epsilon - (\omega_p/\omega_j)^2$.

The subscript $j = 1, 2$ represents the first and second Gaussian laser beam, respectively. The term 'c' is the speed of electromagnetic waves in free space and its value is 3×10^8 m/s^2. The electrons of m-CNTs experience oscillatory behavior due to propagating laser beams. As a result velocity components of the electrons of m-CNTs along the x and z-direction can be written as:

$$v_{jx} = \frac{e\{i(\omega_j + iv)E_{jx} - \omega_c E_{jz}\}}{m\{(\omega_j + iv)^2 - \omega_c^2\}}, \text{ and } v_{jz} = \frac{e\{i(\omega_j + iv)E_{jz} + \omega_c E_{jx}\}}{m\{(\omega_j + iv)^2 - \omega_c^2\}}, \tag{3}$$

where, $\omega_c = eB/m$ is known as the cyclotron frequency of the electrons of m-CNTs and ν represents the collision frequency. The external magnetic field provides anisotropic behavior to the electric permittivity.

The various components of this anisotropic tensor can be calculated as $\epsilon_{jzy} = \epsilon_{jyz} = \epsilon_{jxy} = \epsilon_{jyy} = \epsilon_{jyx} = 0, \epsilon_{jxx} = \epsilon_{jzz} = 1 - \omega_p^2\omega_0/\omega_j\omega_a^2$ and $\epsilon_{jxz} = -\epsilon_{jzx} = -i\omega_c\omega_p^2/\omega_j\omega_a^2$, where $\omega_a^2 = (\omega_0^2 - \omega_c^2)$. The laser beams propagating through the m-CNTs are responsible for static and beat frequency ponderomotive forces acting on the electrons of m-CNTs. Out of these forces, beat frequency ponderomotive force is responsible to generate THz field whereas, the static ponderomotive force experienced by the electrons of m-CNTs is given as:

$$F_{Py} = \sum_{j=1,2} \frac{-e^2}{4m\omega_a^2}\frac{\partial}{\partial y}\left\{E_{jx}E_{jx}^* + E_{jz}E_{jz}^* + \frac{i\omega_c}{\omega_j}\left(E_{jx}E_{jz}^* - E_{jz}E_{jx}^*\right)\right\}. \tag{4}$$

In the state of equilibrium, the pressure gradient force is well counterbalanced by the static ponderomotive force acting along the direction of the applied static magnetic field. Hence, the altered electron density is given by the relation $n = n_0 e^{-\sum_{j=1,2}\rho_j E_{jx}E_{jx}^*}$, where n is known as the altered electron density and n_0 is the electron density of the m-CNTs before the propagation of Gaussian laser beams. The term ρ_j provides the measure of the nonlinearity (due to variation in the ponderomotive force) present in the m-CNTs during the propagation of laser beams and for extraordinary mode ρ_j can be expressed in terms of electronic and ionic temperatures (T_e, T_i) of plasma given as:

$$\rho_j = \frac{e^2}{4mK_B(T_e+T_i)\omega_a^2}\left[1 + \frac{\omega_c^2\{\omega_P^4+2\omega_P^2(\omega_a^2-\omega_P^2\omega_0/\omega_j)\}}{\omega_j^2(\omega_a^2-\omega_P^2\omega_0/\omega_j)^2}\right], \quad (5)$$

In paraxial ray approximation, one can expand the dielectric tensor ε_j as $\epsilon_j = \epsilon_{0j} - \epsilon_{2j}x^2$, where ϵ_{0j} and ϵ_{2j} represent the linear and nonlinear parts of the dielectric function. The wave propagation equation along the x-direction can be written as:

$$\frac{\partial^2 E_{jx}}{\partial z^2} + 2\delta_j\frac{\partial^2 E_{jx}}{\partial x^2} + \frac{\epsilon_{jxz0}}{\epsilon_{jzz0}}\frac{\partial^2 E_{jx}}{\partial x\,\partial z} + \frac{\omega_j^2}{c^2}(\epsilon_{0j} - \epsilon_{2j}x^2)E_{jx} = 0, \quad (6)$$

where, $\epsilon_{jxx0} = \epsilon_{jzz0} = 1 - \omega_P^2\omega_0/\omega_j\omega_a^2$, $\epsilon_{jxz0} = -\epsilon_{jzx0} = -i\omega_c\omega_P^2/\omega_j\omega_a^2$, $\epsilon_{jzz0} \mp \epsilon_{jxz0} = \epsilon_{j0\pm}$, and $\epsilon_{0+}\epsilon_{0-}/(\epsilon_{0+}+\epsilon_{0-})^2 = \delta_j$. The above Eq. (6) can be simplified by assuming that the solution corresponding solution is $E_{jx} = A_j(x,z)e^{-\iota k_j z}$.

According to Akhmanov *et al.* [18], we can express the amplitude in terms of real and imaginary functions as $A_j(x,z)$ as $A_j(x,z) = A_j e^{-\iota k_j S_j(x,z)}$. Where $A_j(x,z)$ and $S_j(x,z)$ are the real function of space. By using the expression for A_j in Eq. (6), we get the resulting equation as:

$$\frac{\partial A_{j0}^2}{\partial z} + 2\delta_j\left(\frac{\partial S_j}{\partial x}\right)\left(\frac{\partial A_{j0}^2}{\partial x}\right) + \frac{\partial^2 S_j}{\partial x^2}A_{j0}^2 = 0, \quad (7)$$

The intensity of Gaussian laser beams in terms of normalized dimensionless beam width parameter (f_j) can be written as $A_{j0}^2 = \left(E_{jx00}^2/f_j\right)e^{-\left(x^2/r_j^2 f_j^2\right)}$. The dimensionless beam width parameter is very significant because it is used to determine the beam width profile of the laser beams, which are propagating through the m-CNTs. The term r_j represents the radii of laser beams. The electric field amplitude is represented as E_{jx00}^2 and the amplitude of eikonal S_j is given as $S_j = (x^2/2)\beta_j(z) + \phi_j(z)$, where $\phi_j(z)$ is the phase factor and $\beta_j(z)$ is known as the wavefront of the laser beam. The value of $\beta_j(z)$ is represented by the relations $\beta_j(z) = (1/2\delta_j f_j)\,\partial f_j/\partial z$. By using these values, the above Eq. (7) can be simplified further to derive the cross-focusing equation of the Gaussian laser beams propagating in the system of m-CNTs.

$$\frac{d^2 f_j}{d\zeta^2} = \frac{4\delta_j^2}{f_j^3} - k_j^2 r_j^4 f_j. \quad (8)$$

where, $\zeta = z/k_j r_j^2$ is known as normalized distance.

The above Eq. (8) reveals the convergence or divergence action of laser beams in the magnetized collisional plasma present in the form of CNTs. The values of ϵ_{0j} and ϵ_{2j} can be obtained by expanding the dielectric relation $\epsilon_j = \epsilon_{0j} - \epsilon_{2j}x^2$ in the paraxial regime around the position of maxima intensity.

Terahertz generation

As explained in part II of the manuscript, the electrons of m-CNTs experience beat frequency ponderomotive force along x and z-direction. Both the components of beat frequency ponderomotive force are eligible to generate THz field and hence THz radiation. These components of the ponderomotive force are given as:

$$F_{PMx} = \frac{e^2E_{1x00}E_{2x00}}{2m(i\omega_1+\nu)(-i\omega_2+\nu)\sqrt{f_1f_2}}\left(1 - \frac{\epsilon_{1xz0}\epsilon_{2xz0}^*}{\epsilon_{1zz0}\epsilon_{2zz0}^*}\right)\left(\frac{x}{r_1^2f_1^2} + \frac{x}{r_2^2f_2^2}\right)\exp\left\{\frac{-x^2}{2}\left(\frac{1}{r_1^2f_1^2} + \frac{1}{r_2^2f_2^2}\right) - i(kz-\omega t)\right\}. \quad (9)$$

$$F_{PMz} = \frac{e^2E_{1x00}E_{2x00}}{2m(i\omega_1+\nu)(-i\omega_2+\nu)\sqrt{f_1f_2}}\left(1 - \frac{\epsilon_{1xz0}\epsilon_{2xz0}^*}{\epsilon_{1zz0}\epsilon_{2zz0}^*}\right)\left\{\left(\frac{1}{2f_1}\frac{df_1}{dz} + \frac{1}{2f_2}\frac{df_2}{dz}\right) - x^2\left(\frac{1}{r_{10}^2f_1^3}\frac{df_1}{\partial z} + \frac{1}{r_{20}^2f_2^3}\frac{df_2}{dz}\right) + ik\right\}\exp\left\{\frac{-x^2}{2}\left(\frac{1}{r_{10}^2f_1^2} + \frac{1}{r_{20}^2f_2^2}\right) - i(kz-\omega t)\right\}. \quad (10)$$

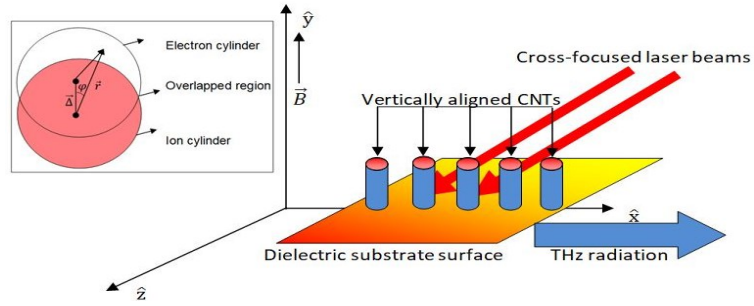

Figure 1 Schematic representation of THz generation and inset figure shows the formation of space charge static field in the overlapped region.

The free plasma electrons of the m-CNTs experience detachment from the ion cylinder and form their separate folk at $\vec{\Delta}$ As a consequence, the space charge electric field is created and this is shown in inset **Figure 1**. Following Kumar *et al.* [8], the net space charge electric field $\vec{E}$ at the point (r, φ, z) is given as:

$$\vec{E} = \frac{n_0 e}{2\epsilon}\left\{(r^2 - a_1^2)\left(\frac{\vec{r}}{r^2}\right) - \left(\left|\vec{r} - \vec{\Delta}\right|^2 - a_1^2\right)\left(\frac{\vec{r}-\vec{\Delta}}{\left|\vec{r}-\vec{\Delta}\right|^2}\right)\right\}. \quad (11)$$

The displacement of the electrons parallel to the CNT axis is zero but non-zero along the perpendicular direction (x-axis). Therefore, the expression of the x-component of the space charge electric field and the restoring force for the electrons of the m-CNTs can be given as:

$$F_x = \frac{-n_0 e^2}{2\epsilon}\left\{\left(1 + \frac{a_1^2}{r^2}\right)\Delta_x + \left(\frac{5\cos\varphi}{r} + \frac{4\cos^2\varphi}{r} - \frac{(r^2 - a_1^2)\cos\varphi}{r^3}\right)\right\}\Delta_x^2. \quad (12)$$

As the restoration force for the different electrons of m-CNTs is not the same, therefore we have to calculate the average value of restoration force over φ and r. The average restoration force is given as:

$$\langle F_x \rangle = \frac{-m\omega_P^2}{2\epsilon_r}\Delta_x[1 + \beta + \alpha\Delta_x], \quad (13)$$

where, $\beta = 2\,a_1^2 \log_e(a_2/a_1)\,/(a_2^2 - a_1^2)$ is known as a characteristic parameter and $\alpha = 4/(a_2 + a_1)$ is known as anharmonicity factor. Both β and α are linked with the anharmonic behavior of m-CNTs. The equations governing the displacement of the electrons of CNTs in the presence of space charge restoration force, Ponderomotive force, and magnetic force is given as:

$$\frac{d^2\Delta_x}{dt^2} + \frac{\omega_P^2}{2\epsilon_r}(1 + \beta + \alpha\Delta_x)\Delta_x + \nu\frac{d\Delta_z}{dt} - \frac{eB}{m}\frac{d\Delta_z}{dt} = -\frac{F_{PMx}}{m}. \quad (14)$$

$$\frac{d^2\Delta_z}{dt^2} + \nu\frac{d\Delta_z}{dt} + \frac{eB}{m}\frac{d\Delta_x}{dt} = -\frac{F_{PMz}}{m}. \quad (15)$$

By solving Eqs. (14) - (15), one can find the value of Δ_z and Δ_x. The expressions for these displacements can be written as:

$$\Delta_z = \frac{\left[1 - \{(1+\beta)\omega_P^2/2\omega^2\epsilon_r\} + (i\upsilon/\omega)\right] F_{PMz} - (\omega_c/\omega)F_{PMx}}{m\omega^2\{1 + (i\upsilon/\omega)\}\left[1 - \{(1+\beta)\omega_P^2/2\omega^2\epsilon_r\} + (i\upsilon/\omega) - [\omega_c^2/\omega^2\{1 + (i\upsilon/\omega)\}]\right]}. \text{ and}$$

$$\Delta_x = \frac{\{1 + (i\upsilon/\omega)\}F_{PMx} + i(\omega_c/\omega)\,F_{PMz}}{m\omega^2\{1 + (i\upsilon/\omega)\}\left[1 - \{(1+\beta)\omega_P^2/2\omega^2\epsilon_r\} + (i\upsilon/\omega) - [\omega_c^2/\omega^2\{1 + (i\upsilon/\omega)\}]\right]}. \quad (16)$$

Corresponding to these displacements of plasma electrons of the m-CNTs, one can calculate the oscillatory velocities by using the relations $v_x = -i\omega\Delta_x$ and $v_z = -i\omega\Delta_z$.

$$v_x = \frac{-i\omega\{1+(i\upsilon/\omega)\}F_{PMx}+i(\omega_c/\omega)\,F_{PMz}}{m\omega^2\{1+(i\upsilon/\omega)\}\left[1-\{(1+\beta)\omega_P^2/2\omega^2\epsilon_r\}+(i\upsilon/\omega)-\left[\omega_c^2/\omega^2\{1+(i\upsilon/\omega)\}\right]\right]}, \text{ and}$$

$$v_z = \frac{-i\omega\left[1-\{(1+\beta)\omega_P^2/2\omega^2\epsilon_r\}+(i\upsilon/\omega)\right]F_{PMz}-(\omega_c/\omega)\,F_{PMx}}{m\omega^2\{1+(i\upsilon/\omega)\}\left[1-\{(1+\beta)\omega_P^2/2\omega^2\epsilon_r\}+(i\upsilon/\omega)-\left[\omega_c^2/\omega^2\{1+(i\upsilon/\omega)\}\right]\right]}. \quad (17)$$

The nonlinear current density corresponding to the oscillatory velocity of CNT electrons can be expressed by using the relation $J^{NL} = -evn_{\rho 0}e^{-i\rho z}$, where $n_{\rho 0}$ is known as the amplitude and ρ as the wavenumber of the ripple density. This current density has a finite value over the cross-sectional surface area of m-CNTs whereas it becomes null over the gap between the m-CNTs. The gap is denoted by the area d^2. As a result, one has to calculate the average value of the THz nonlinear current density. The x and z components of average nonlinear current density are given:

$$J_x^{NL} = \frac{i\pi(a_2^2-a_1^2)N_c e n_{\rho 0}[\{1+(i\upsilon/\omega)\}F_{PMx}+i(\omega_c/\omega)\,F_{PMz}]}{m\omega\{1+(i\upsilon/\omega)\}\left[1-\{(1+\beta)\omega_P^2/2\omega^2\epsilon_r\}+(i\upsilon/\omega)-\left[\omega_c^2/\omega^2\{1+(i\upsilon/\omega)\}\right]\right]}, \text{ and}$$

$$J_z^{NL} = \frac{i\pi(a_2^2-a_1^2)N_c e n_{\rho 0}\left[\left[1-\{(1+\beta)\omega_P^2/2\omega^2\epsilon_r\}+(i\upsilon/\omega)\right]F_{PMz}-(\omega_c/\omega)\,F_{PMx}\right]}{m\omega\{1+(i\upsilon/\omega)\}\left[1-\{(1+\beta)\omega_P^2/2\omega^2\epsilon_r\}+(i\upsilon/\omega)-\left[\omega_c^2/\omega^2\{1+(i\upsilon/\omega)\}\right]\right]}. \quad (18)$$

The above calculated nonlinear current density J_x^{NL} provides its significant contribution to the THz generation and it is obvious from the following standard wave propagation equation (derived from Maxwell's equations) used to explain the THz dynamics:

$$\nabla^2\vec{E} - \nabla\left(\nabla.\vec{E}\right) = \frac{4\pi}{c^2}\frac{\partial}{\partial t}\left(\vec{J}^{NL}\right) + \frac{1}{c^2}\frac{\partial^2\vec{E}}{\partial t^2}, \quad (19)$$

where, $\vec{E}$ is the THz field which varies as $\vec{E} = \hat{x}\vec{E}_{x0}(x,t)e^{-i(kz-\omega t)}$. We can solve the above Eq. (19) with the help of Eqs. (18a) - (18b), by neglecting the term $\nabla\left(\nabla.\vec{E}_T\right)$ and using the phase-making condition which demands that:

$$k=\frac{\omega}{c}\sqrt{1-\frac{\omega_P^2}{\omega^2}\left[\frac{\{1+(i\upsilon/\omega)\}-(\omega_P^2/\omega^2)}{\{1+(i\upsilon/\omega)\}[\{1+(i\upsilon/\omega)\}-(\omega_P^2/\omega^2)]-(\omega_c^2/\omega^2)}\right]}. \quad (20)$$

Finally, the normalized equation for the THz electric field amplitude can be obtained as:

$$4i\frac{\partial}{\partial\zeta}\left(\frac{E_{x0}}{E_{2x00}}\right) + 2\left(\frac{k_1}{k}\right)r_1^2\left[k^2 - \frac{\omega^2}{c^2} + \frac{\omega_P^2}{c^2}\left[\frac{\{1+(i\upsilon/\omega)\}-(\omega_P^2/\omega^2)}{\{1+(i\upsilon/\omega)\}[\{1+(i\upsilon/\omega)\}-(\omega_P^2/\omega^2)]-(\omega_c^2/\omega^2)}\right]\right] =$$
$$\pi(a_2^2-a_1^2)N_c\{1+(i\upsilon/\omega)\}^{-1}\left(\frac{n_{\rho 0}}{n_0}\right)\left(\frac{\omega_P^2}{\omega^2}\right)\left[1-\{(1+\beta)\omega_P^2/2\omega^2\epsilon_r\}+(i\upsilon/\omega)-\right.$$
$$\left.[\omega_c^2/\omega^2\{1+(i\upsilon/\omega)\}]\right]^{-1}\left(\frac{eE_{2x00}}{m\omega c}\right)\left(\frac{\omega}{\omega_1}\right)\left(\frac{\omega}{\omega_2}\right)\frac{\{1-(i\upsilon/\omega_1)\}^{-1}\{1+(i\upsilon/\omega_2)\}^{-1}}{\sqrt{f_1 f_2}}\left(1-\frac{\epsilon_{1xz0}\epsilon_{2xz0}^*}{\epsilon_{1zz0}\epsilon_{2zz0}^*}\right)\left[\frac{1}{S_3}\left\{\left(\frac{S_1x_1}{kr_1f_1^2}+\frac{S_1x_2}{kr_2f_2^2}\right)+\right.\right.$$
$$\left.\left.\left\{\left(\frac{S_2}{2(kr_1)(k_1r_1)f_1}\frac{df_1}{d\zeta}+\frac{S_2}{2(kr_2)(k_1r_2)f_2}\frac{df_2}{d\zeta}\right)-\left(\frac{x_1^2}{f_1^3(kr_1)(k_1r_1)}\frac{df_1}{\partial\zeta}+\frac{x_2^2}{f_2^3(kr_2)(k_1r_2)}\frac{df_2}{d\zeta}\right)+i\right\}\right\}\right], \quad (21)$$

where, $S_1 = \{1+(i\upsilon/\omega)\}\left(\{1+(i\upsilon/\omega)\}^2-\frac{\omega_c^2}{\omega^2}\right)-\frac{\omega_P^2}{\omega^2}\left(\{1+(i\upsilon/\omega)\}^2-\frac{i\omega_c^2}{\omega^2}\right)$, $S_2 = \left[\frac{i\omega_c}{\omega}\left\{\{1+(i\upsilon/\omega)\}^2-\frac{\omega_c^2}{\omega^2}\right\}-\frac{\omega_P^2}{\omega^2}\{1+(i\upsilon/\omega)\}\right]-i\left(\frac{\omega_c}{\omega}\right)\left(\frac{\omega_P^2}{\omega^2}\right)\left[1-\frac{\omega_P^2(1+\beta)}{2\omega^2\epsilon_r}+\frac{i\upsilon}{\omega}\right]$, $S_3 = \left[\{1+(i\upsilon/\omega)\}^2-\frac{\omega_c^2}{\omega^2}\right]-\frac{\omega_P^2}{\omega^2}\{1+(i\upsilon/\omega)\}$, $x_1 = x/r_1$, and $x_2 = x/r_2$.

By applying appropriate boundary conditions, one can solve the above Eq. (21) to obtain the THz field amplitude of emitted THz radiation.

Results and discussion

One can solve Eq. (8) numerically by using Runge-Kutta (RK) method. For this purpose, 2 initial conditions have been used. The first condition is given as $f_1|_{\zeta=0} = f_2|_{\zeta=0} = 1$. The first order derivative of the first condition with respect to normalized distance ζ provides the second condition given as $\frac{df_1}{d\zeta}\Big|_{\zeta=0} = \frac{df_2}{d\zeta}\Big|_{\zeta=0} = 0$. The threshold power for cross-focusing can be obtained by using the

conditions $\left.\frac{df_1}{d\zeta}\right|_{\zeta=0}$, $f_1|_{\zeta=0} = 1$ and $\left.\frac{df_2}{d\zeta}\right|_{\zeta=0}$, $f_2|_{\zeta=0} = 1$ for the various values of normalized distance ζ. For the powers above the threshold, one can use the condition of second order derivative given as $\frac{d^2 f_1}{d\zeta^2} < 0$. To carry out the numerical computation and analysis, we have used the specific set of laser-plasma and CNT parameters: $\omega_1 = 2.40 \times 10^{14}\ \text{rads}^{-1}$, $\omega_2 = 2.10 \times 10^{14}\ \text{rads}^{-1}$, $\lambda_1 = 0.800\ \mu\text{m}$, $\lambda_2 = 0.700\ \mu\text{m}$, the intensity of laser beams $I_1 \sim I_2 = 10^{14}\ \text{Wcm}^{-2}$, radii of the laser beams $r_1 = 20.00\ \mu\text{m}$ and $r_2 = 40.00\ \mu\text{m}$. The inner and outer radii of CNTs are 40.00 and 80.00 nm, respectively. The inter-tube separation between the CNTs is $d = 60.00$ nm in the array. **Figures 2(a)** and **2(b)** represent the numerical results for cross-focused laser beams in the collisional plasma of m-CNTs under the action of the applied static magnetic field. In **Figure 2(a)**, the variation of dimensionless beam width parameters f_1 has been shown with normalized distance ζ and in **Figure 2(b)**, the variation of dimensionless beam width parameters f_2 has been shown with normalized distance ζ. The **Figure 2(a)** and **2(b)** both shows the converging and diverging behavior of the laser beams propagating through the m-CNTs. It is clear from the Figure. that beam width parameter f_1 and f_2 decreases as the laser beams propagate and attain a minimum value at a particular value of normalized distance ζ. After attaining the minimum value, beam width parameters f_1 and f_2 start increasing again. This is because diffraction becomes more dominating than the nonlinear refraction effect. This behavior is in accordance with Eq. (8). From the **Figures 2(a)** and **2(b)**, it is also observed that the focusing of both laser beams gets affected by the change in the value of the externally applied static magnetic field (100, 200 and 300 kG). The focusing of each beam shows a significant increase with the increasing magnetic field and attains peak value, at the optimized value of the magnetic field. This is because of the increase in the ponderomotive nonlinearity in the direction of the applied static magnetic field. The expected uncertainty in the dimensionless beam width parameter f_1 and f_2 at the optimized value of the externally applied static magnetic field (300 kG) is of the order of ~75 and ~65 %, respectively.

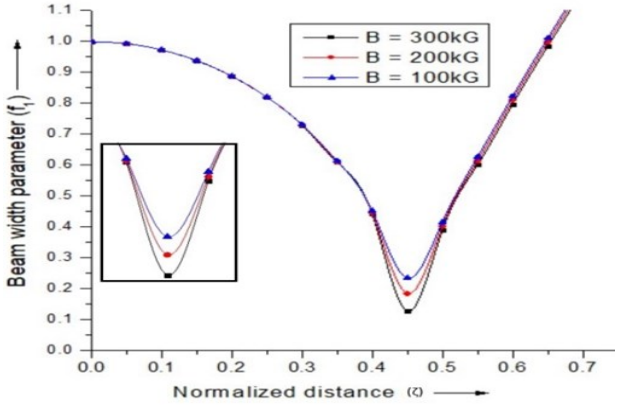

(a)

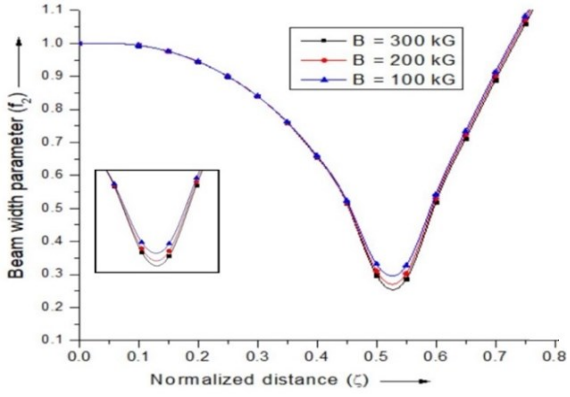

(b)

Figure 2 (a) Variation of dimensionless beam width parameter f1 with normalized distance ζ, at various values of the static magnetic field, and (b) Variation of dimensionless beam width parameter f2 with normalized distance ζ, at various values of the static magnetic field.

Figure 3 shows the variation of normalized THz amplitude with normalized distance (x/r_1) at different values of static magnetic field $(100, 200 \text{ and } 300 \text{ kG})$. From the curves, it is observed that the normalized THz amplitude increases firstly, along the direction of propagation of lasers and then attains maximum value. After attaining maximum value, it begins to decrease. The physics behind such a behavior can be explained as follows. The ponderomotive nonlinearity along the direction of static magnetic field and collisions between the electrons makes the focusing of lasers more strong that leads to enhancement of the intensity of 2 lasers. The increase in the normalized THz amplitude is because of this increased intensity of lasers. However, a further increase in the intensity of lasers increases the nonlinear ponderomotive force. This force repels the electrons out of the axial region and as a result, THz amplitude shows a decrease. The external static magnetic field enhances the normalized THz amplitude to large extent. It is because, with the increase of the static magnetic field, ponderomotive nonlinearity also increases.

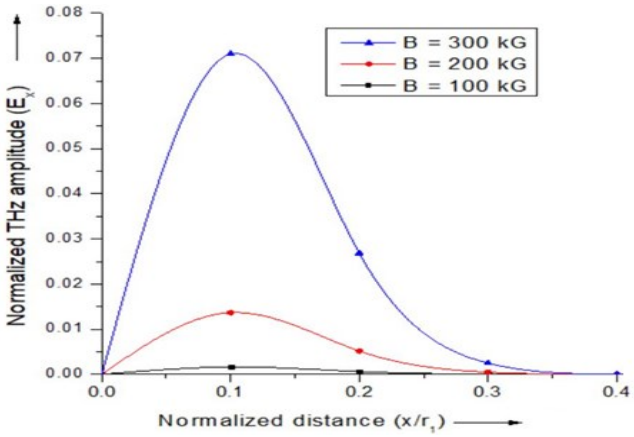

Figure 3 Variation of normalized THz amplitude with normalized distance (x/r_1) at various values of the static magnetic field

Figure 4 shows the variation of normalized THz wave amplitude with and without the effect of cross focusing of the laser beams at the optimized value of static magnetic field (300 kG). The other parameters are kept the same as that in **Figure 3**. From the plots of **Figure 4**, one can observe that the normalized THz field amplitude is ~ 0.005 in the absence of the cross-focusing and it increases to ~ 0.07 in the presence of cross-focusing in the m-CNTs. Approximately 14 times increase is observed in the normalized THz amplitude with the effect of cross focusing of lasers as compared to without cross focusing. This is on account of the fact that the cross focusing of the lasers leads to the increase in the intensity of the laser, Which further results in the increase of the ponderomotive nonlinearity. The cross-focusing effect of co-propagating Gaussian laser beams facilitates the THz generation in the m-CNTs by enhancing the THz field. Therefore, cross focusing plays a significant role in the enhancement of the normalized THz amplitude.

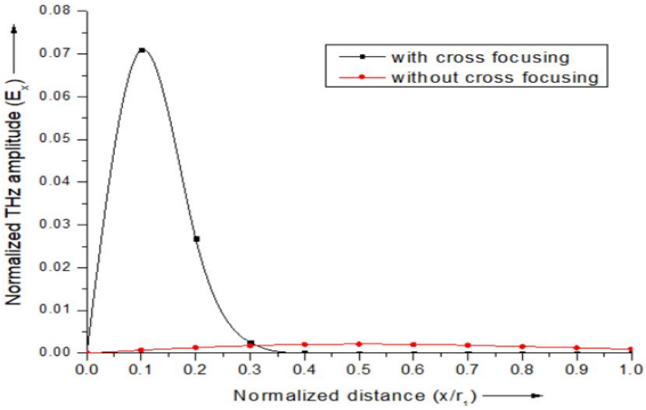

Figure 4 Normalized THz amplitude Variation with and without cross focusing of laser beams, with normalized distance (x/r_1) at the optimized value of static magnetic field (300 kG).

In **Figure 5**, we have plotted variation of normalized THz amplitude with normalized distance for various values of outer radii of CNTs, keeping the inner radius constant at the optimized value of externally applied static magnetic field (300 kG). The other parameters are kept the same as that in **Figure 3**. From the graph, it is clear that the normalized THz wave amplitude attains the peak value at a higher value of the outer radius of CNTs. This is because of the increase in the nonlinearities of the vertical array of m-CNTs behaving as plasma. As the generation of THz radiation is also known as the nonlinear phenomenon, therefore enhancement of the normalized THz amplitude is obvious.

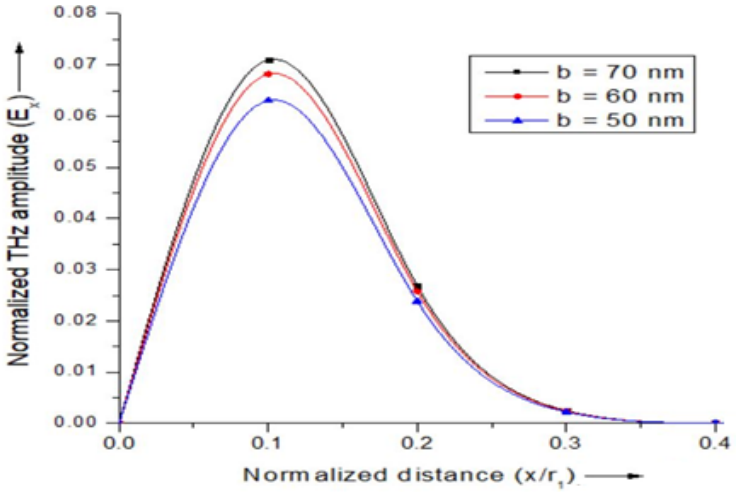

Figure 5 Variation of normalized THz amplitude with normalized distance (x/r_1) for various values of the outer radii of CNTs at the optimized value of externally applied static magnetic field (300 kG).

In **Figure 6**, we have shown the variation of normalized THz wave amplitude with normalized distance for various values of inter-tube separation in the array at the optimized value of externally applied static magnetic field (300 kG). All other parameters are kept the same as that in **Figure 3**. From the graph it is observed that the normalized THz wave amplitude decreases with the increase of the inter-tube separation. This is because of the increase in the nonlinearities in the m-CNTs, due to the more absorption of the lasers by these m-CNTs. This result is also in accordance with Kumar *et al.* [22], in which they applied cross-focusing to enhance THz generation in the array of CNTs.

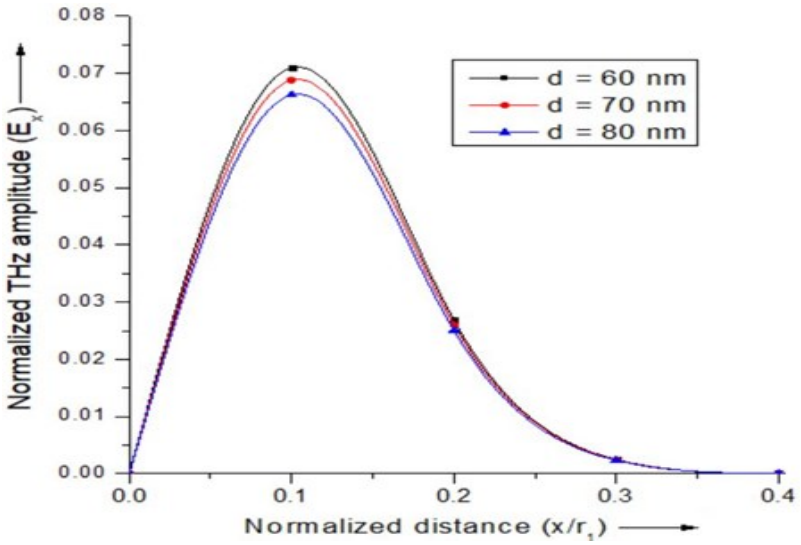

Figure 6 Variation of normalized THz amplitude with normalized distance(x/r_1) for various values of inter-tube separation distance (d) at the optimized value of externally applied static magnetic field (300 kG).

Conclusions

In the proposed scheme, the THz electric field has been generated by using the cross focusing of 2 Gaussian laser beams in the array of vertically aligned m-CNTs grown over the dielectric substrate. In this scheme, the effect of cross-focusing enhances the normalized THz electric field amplitude by 14 times as compared to the THz electric field amplitude in the absence of cross-focusing, which is better than others. The cross-focusing effect of co-propagating Gaussian laser beams facilitates the THz generation in the m-CNTs by enhancing the THz field. It is observed that the focusing of each laser beam depends upon the applied static magnetic field $\left(\vec{B} = 100, 200 \text{ and } 300 \text{ kG}\right)$ and intensity of each incident Gaussian laser beam($I_1 \sim I_2 = 10^{14}\ \text{Wcm}^{-2}$). During the cross-focusing of laser beams, there occurs maximum energy transfer from the laser beams to the emitted THz radiations. The normalized THz amplitude shows significant enhancement with the increase of cross-focusing as compared to the case without cross-focusing. The enhancement is also observed in the THz amplitude with the variation of internal and external diameters of m-CNTs. THz radiations emitted in this way can prove to be beneficial in the biological diagnosis (of the living beings) instead of X-rays. In the future, we can also extend this work by applying the static magnetic field transverse to the longitudinal axis of the CNTs to observe the effect on the THz field of emitted radiations.

References

[1] B Ferguson and XC Zhang. Materials for terahertz science and technology. *Nat. Mater.* 2002; **1**, 26-30.

[2] PH Siegel. Terahertz technology in biology and medicine. *IEEE Trans. Micro. Theor. Tech.* 2004; **52**, 2438.

[3] M Tonouchi. Cutting-edge THz technology. *Nat. Photon.* 2007; **1**, 97-102.

[4] JB Jackson, M Mourou, JF Whitaker, IN Duling, SL Williamson, M Menu and GA Mourou. Terahertz imaging for non-destructive evaluation of mural painting. *Opt. Commun.* 2008; **281**, 527-32.

[5] J Federici and L Moeller. Review of terahertz and subterahertz wireless communications. *J. Appl. Phys.* 2010; **107**, 111101.

[6] S Kumar, S Vij, N Kant and V Thakur. Nonlinear interaction of amplitude-modulated Gaussian Laser beam with anharmonic magnetized and rippled CNTs: THz generation. *Braz. J. Phys*. 2023; **53**, 37.

[7] S Kumar, S Vij, N Kant and V Thakur. Interaction of spatial-Gaussian lasers with the magnetized CNTs in the presence of D.C electric field and enhanced THz emission *Phys. Scr.* 2023; **98**, 015015.

[8] S Kumar, S Vij, N Kant and V Thakur. Resonant terahertz generation by the interaction of laser beams with magnetized anharmonic carbon nanotube array. *Plasmonics* 2021; **17**, 381-8.

[9] S Kumar, S Vij, N Kant and V Thakur. Resonant excitation of THz radiations by interaction of amplitude-modulated lasers with an anharmonic CNTs in the presence of static D.C. electric and magnetic fields *Chin. J. Phys*. 2022; **78**, 453-62.

[10] V Thakur, S Vij, N Kant and S Kumar. THz generation by propagating lasers in magnetized SWCNTs. *Indian J. Phys.* 2023. https://doi.org/10.1007/s12648-022-02575-x

[11] S Kumar, S Vij, N Kant and V Thakur. Interaction of obliquely incident lasers with anharmonic CNTs acting as dipole antenna to generate resonant THz radiation. *Waves Random Complex Media* 2022. https://doi.org/10.1080/17455030.2022.2155330

[12] LV Titova, CL Pint, Q Zhang, RH Hauge, J Kono and FA Hegmann. Generation of terahertz radiation by optical excitation of aligned carbon nanotubes. *Nano Lett.* 2015; **15**, 3267.

[13] S Kumar, S Vij, N Kant, A Mehta and V Thakur. Resonant terahertz generation from laser filaments in the presence of static electric field in magnetized collisional plasma. *Eur. Phys. J. Plus* 2021; **136**, 148.

[14] S Kumar, S Vij, N Kant and V Thakur. Combined effect of transverse electric and magnetic fields on THz generation by beating of two amplitude-modulated laser beams in the collisional plasma. *J. Astrophys. Astr.* 2022; **43**, 30.

[15] M Abedi-Varaki and S Jafari. Enhanced THz radiation from beating of two Cosh-Gaussian laser beams in a wiggler-assisted collisional magnetized plasma. *J. Opt. Soc. Am. B* 2018; **35**, 1165-72.

[16] M Abedi-Varaki. Enhanced THz radiation generation by photo-mixing of tophat lasers in rippled density plasma with a planar magnetostatic wiggler and s-parameter. *Phys. Plasma.* 2018; **25**, 023109.

[17] RP Sharma and RK Singh. Terahertz generation by two cross focused laser beams in collisional plasmas. *Phys. Plasma.* 2014; **21**, 073101.
[18] SA Akhmanov, AP Sukhorukov and RV Khokhlov. Self-focusing and diffraction of light in a nonlinear medium. *Sov. Phys. Usp.* 1968; **10**, 609.
[19] AK Sharma. Transverse self-focusing and filamentation of a laser beam in a magnetoplasma. *J. Appl. Phys.* 1978; **49**, 2396.
[20] V Thakur, N Kant and S Vij. Effect of cross-focusing of two laser beams on THz radiation in graphite nanoparticles with density ripple. *Phys. Scripta* 2020; **95**, 045602.
[21] S Kumar, N Kant and V Thakur. THz generation by self-focused Gaussian laser beam in the array of anharmonic VA-CNTs. *Opt. Quant. Electron.* 2023; **55**, 281.
[22] S Kumar, S Vij, N Kant and V Thakur. Resonant terahertz generation by cross-focusing of Gaussian laser beams in the array of vertically aligned anharmonic and magnetized CNTs. *Opt. Commun*. 2022; **513**, 128112.